Zhang, S. Y., Neild, S., & Jiang, J. Z. (2020). Optimal design of a pair of vibration suppression devices for a multi-storey building. *Structural Control and Health Monitoring*, *27*(3), [e2498]. https://doi.org/10.1002/stc.2498

STRUCTURAL CONTROL AND HEALTH MONITORING
Struct. Control Health Monit. 2015; **00**:1–20
Published online in Wiley InterScience (www.interscience.wiley.com). DOI: 10.1002/stc

Optimal design of a pair of vibration suppression devices for a multi-storey building

Sara Ying Zhang[1,2], Simon Neild[2] and Jason Zheng Jiang[2,*,†]

[1]*Institute of Urban Smart Transportation & Safety Maintenance, Shenzhen University, Shenzhen, China*
[2]*Department of Mechanical Engineering, University of Bristol, Bristol, UK*

SUMMARY

This paper investigates the use of two two-terminal vibration suppression devices in a building and assesses the performance benefits over those achieved using a single device. The inerter-combined configurations for a multi-storey building structure are considered. The inerter is a two-terminal device, with the property that the applied force is proportional to the relative acceleration across its terminals. In this paper, a five-storey building model with two absorbers of the same kind subjected to base excitation is studied, where one is located between ground and the first floor and the other is between the first and second floors of the building. Three passive suppression layouts, two dampers, two tuned inerter dampers and two tuned viscous mass dampers, are considered. The optimal configurations for minimising the maximum inter-storey drifts of the building are obtained with respect to the inerter's size and the damping boundary. The corresponding parameter values are also presented. For the sake of comparison, the single device mounted between the ground and first floor is also considered. Finally, with specific inertance and damping values, the frequency response is provided to show the potential advantage of the proposed optimal configurations. It is demonstrated that the optimal configurations with a pair of devices is more effective than the optimal single device with equal total inertance and the same total damping boundary. The approach demonstrated in this paper is applicable to the investigation of using more than two devices for multi-storey buildings.

Received . . .

KEY WORDS: Inerter; vibration suppression; a pair of absorbers; base excitation; structural control

1. INTRODUCTION

Human safety and comfort are two main concerns for dynamic design of building structures. The tuned mass damper (TMD) proposed by Frahm [1] has been widely accepted as an effective passive control device. Den-Hartog [2] proposed and others [3–5] have refined the tuning method to choose the damping ratio of the TMD to maximize energy dissipation. Considering the motion of the structure as well as that of the TMD, Krenk [6] characterised the damping properties and identified the optimal damping of TMD. In most real applications, only a single TMD is used and it is always installed near the top of the building, see for example the analysis in [7, 8]. To investigate the performance of multiple TMDs, Iwanami and Seto [9] proposed dual tuned mass dampers (2TMD) for suppressing the vibration of a single degree of freedom (SDOF) structure with harmonically forced oscillation and it was shown that 2TMD are more effective than a single TMD. Deploying multiple tuned mass dampers (MTMD) in a structure has also been studied in [10–15], which concluded that MTMD can result in a better performance than a single TMD with the same total

*Correspondence to: Jason Zheng Jiang, Department of Mechanical Engineering, University of Bristol, Bristol, UK.
†E-mail:z.jiang@bristol.ac.uk

mass. In [16], Rana and Soong investigated the control of multiple structural modes with MTMD located between the different floors in a MDOF building. Xiang and Nishitani [17] proposed the TMD floor system (TMDFS) which takes advantages of both the floor isolation system (FIS) and TMD. Using the multimode approach, it has been shown that a structure with several TMD floors can perform better than one with a single TMD floor. For multiple dampers, Takewaki [18] proposed an efficient and systematic procedure for finding the optimal placement of the dampers.

The inerter is a two-terminal device, introduced by Smith [19] in the early 2000s, which has the property that the force generated by it is proportional to the relative acceleration across its terminals. The inerter completes the force-current analogy between mechanical and electrical networks with the inerter corresponding to the capacitor, the spring corresponding to the inductor and the damper corresponding to the resistor. The performance advantages of various mechanical systems incorporating inerters have been identified in [20–29]. The application of inerter-based suppression systems in buildings has also been analysed by many researchers as the inerter can provide a high inertance with a much lower mass due to internal gearing. In 2010, Wang *et al.* [30] proposed several simple inerter-combined absorber layouts that have been shown to be effective in reducing vibration of a one DOF and a two DOF building models. A new inerter-based device, the tuned viscous mass damper (TVMD), was presented by Ikago *et al.* [31] as a vibration suppression device for a SDOF system. In 2013, Lazar *et al.* [32] proposed a tuned inerter damper (TID) by substituting the mass of the widely used TMD with an inerter. The study showed that the performance with a TID mounted between the structure and the ground can be better than that with a TMD mounted at the top of the structure. A tuned mass damper inerter (TMDI) consisting of an inerter mounted in series with a TMD has been proposed in [33]. In [34], the effect of the size of inerter and the stiffness of the brace that links the device across floors, on the optimal inerter-based device layout was considered. They reported three optimal layouts across the inertance-brace stiffness parametric space; the D (damper), the IPD (inerter in parallel with damper) and the TID (tuned inerter damper). It was also noted that beyond a certain value of inertance, a suppression device becomes suboptimal regardless of which layout is used. All these applications focused on using one inerter-based control device in a building structure. In addition, the effect of the inertial mass damper for cables has also been studied in [35, 36].

In [37], TVMDs were mounted within every storey in a multi-storey building and Takewaki *et al.* [38] investigated the earthquake response reduction with inerter-like devices known as inertial dampers used between several floors of a building. Also in 2016, Giaralis and Marian [39] studied the benefits of the TMDIs over the traditional TMDs in a linear building structure. These studies are based on a specific pre-determined layout for the suppression device. As a first step towards multiple inerter-based device investigation, considering two devices makes it easier to interpret the obtained results, and understand the influence of using more than one inerter-based device for vibration suppression in a building model. In addition, it is preferable to use fewer devices from cost and maintenance points of view. In this paper, multiple layouts that have all been shown to be effective as a single device will be compared for the case where a pair of devices is used. In considering their effectiveness, both performance and device size are discussed. Many cost functions could be selected for the optimisation [40]; herein the inter-storey drifts are selected as the performance index. Three candidate layouts — two dampers, TVMDs or TIDs — are considered as the suppression devices, with one device located between the ground and first floor and the other mounted between the first and second floors of the building. In order to scale the device in the same way as is done by selecting the mass ratio for a TMD, the total inertance of the layouts is selected before optimisation. Considering the implementation and potential cost implications, the upper limit of the total damping value is also fixed during optimisation. By optimising the objective function, the optimum results and the corresponding parameter values of different layouts can be obtained with respect to the inerter's size and the damping boundary. Other performance measures and constraints can also be adopted for optimisation, for example, the weight-normalised device forces. However, since the focus of this work is on the optimum vibration absorber methodology, which can be adopted for any performance constraint consideration, we do not pursue these other possible metrics/constraints in this work.

DOI: 10.1002/stc

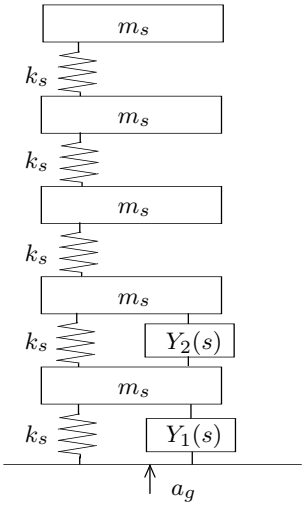

Figure 1. Schematic representation of an idealised building and lower floor suppression device.

This paper is arranged as follows. In Section 2, we introduce an idealised five-storey building model and the optimisation procedure used in the paper. The candidate suppression device layouts are also proposed. In Section 3, optimisation without restricting the damping value is carried out to show the limitation of fixed-sized-inerter method. The optimisation results with respect to the inerter's size and the damping boundary are obtained in Section 4. Conclusions are drawn in Section 5.

2. BUILDING MODEL WITH CANDIDATE VIBRATION SUPPRESSION LAYOUTS AND OPTIMISATION PROCEDURE

In this section, a five storey building model with two absorbers is introduced, where one device is located in the bottom storey and the other one is mounted between the first and second floors as shown in Figure 1. The objective function and the optimisation approach are also provided. Three candidate layouts with two vibration suppression devices of the same kind are considered. Note, we define layouts as the topological arrangements formed by specific connections of springs, dampers and inerters, while the configurations mean the layouts with element values specified.

2.1. Multi-storey building model with general suppression devices

In the present paper, we consider a five storey building model with equivalent floor mass m_s and equivalent inter-storey elasticity k_s, shown in Figure 1, in which the structural damping is taken to be zero because its value is typically small compared with the control device. The locations of the two absorbers are taken to be between the ground and the first, and the first and the second floors, defined as Device1 and Device2, respectively. The control system can be assumed to be passive mechanical admittance $Y(s) = F(s)/v(s)$ [20, 41], where $F(s)$ is the force exerted by the control device in the Laplace domain and $v(s)$ is the relative velocity between the two terminals, also in the Laplace domain. $Y_1(s)$ and $Y_2(s)$ shown in Figure 1 are the general admittances of the two absorbers. The parameters of the five storey building model are fixed as $m_s = 1000\,\mathrm{kg}$ and $k_s = 1500\,\mathrm{kN/m}$. These numerical values were selected for convenience while retaining realistic natural frequencies and noting that the parameters scale linearly.

Defining the variable matrix

$$x = \begin{bmatrix} x_1 & x_2 & x_3 & x_4 & x_5 \end{bmatrix}^T$$

where x_i $(i = 1, \cdots, 5)$ is the displacement of the i-th floor relative to the ground. For the building model of Figure 1, excited by a ground acceleration a_g, we can obtain its equation of motion in

DOI: 10.1002/stc

matrix form, in the Laplace domain as

$$Ms^2X + KX + \delta KX = -MEA_g, \tag{1}$$

where $M = m_sI$ is the 5×5 mass matrix of the structure, where I is the identity matrix, E is a 5×1 vector of ones, X and A_g represent the vector of relative floor displacements and ground acceleration in the Laplace domain and

$$K = \begin{bmatrix} 2k_s & -k_s & 0 & 0 & 0 \\ -k_s & 2k_s & -k_s & 0 & 0 \\ 0 & -k_s & 2k_s & -k_s & 0 \\ 0 & 0 & -k_s & 2k_s & -k_s \\ 0 & 0 & 0 & -k_s & k_s \end{bmatrix}$$

,

$$\delta K = \begin{bmatrix} s(Y_1(s) + Y_2(s)) & -sY_2(s) & 0 & 0 & 0 \\ -sY_2(s) & sY_2(s) & 0 & 0 & 0 \\ 0 & 0 & 0 & 0 & 0 \\ 0 & 0 & 0 & 0 & 0 \\ 0 & 0 & 0 & 0 & 0 \end{bmatrix}$$

.

2.2. Optimisation Procedure and Candidate Vibration Suppression Layouts

Many design criteria for a vibration absorber are proposed in [40], such as limiting the absolute displacement or the absolute acceleration. We consider the inter-storey drift of each floor as the performance index in this paper, as potential damage of a building structure is strongly correlated with the values of inter-storey drifts. Thus the objective for the optimisation of device parameters in this study is to reduce the maximum magnitude of the frequency response functions (FRFs) of the inter-storey drifts among all the floors, with the objective function defined as

$$J_\infty = \max_i \left(\max_\omega |T_{A_g \to Z_i}(j\omega)| \right) \tag{2}$$

where $Z_i = X_i - X_{i-1}$ and $X_0 \equiv 0$. $T_{A_g \to Z_i}$ denotes the transfer function from ground acceleration A_g to inter-storey drift Z_i and $\max\ |T_{A_g \to Z_i}(j\omega)|$ represents the maximum magnitude of $T_{A_g \to Z_i}$ across all frequencies. We note that most real-world ground accelerations are focused on low frequencies under 10 Hz; although the infinity norm can be focused on high frequencies, for the building model considered in this paper, the maximum inter-storey drift always occurs at the first fundamental frequency, around 1.7 Hz, which can be seen from, for example, Figures 16 and 20 in Section 5. The objective function taken here is the same as that proposed by Xiang and Nishitani [17, 42]. The optimisation problem herein can be formulated as to make objective function J_∞ as small as possible. The *patternsearch* and *fminsearch* functions in MATLAB are used in this paper to find the optimum value of J_∞. While the effectiveness of these optimisation algorithms depends on a proper choice of initial values, but these algorithms are faster than global optimisation methodologies that need no initial values (e.g. generic algorithms). To avoid getting stuck at local minima, 10 sets of random initial values, uniform in appropriate ranges, are used for each optimisation and the result with minimum objective function J_∞ is used.

Figure 2 illustrates the four kinds of passive suppression devices: (a) a traditional damper (D); (b) a tuned viscous mass damper (TVMD) [31], (c) a tuned inerter damper (TID) [32] and (d) an inerter with a parallel connected damper (IPD, a special case of TVMD) [34]. The mechanical admittance $Y(s)$ for these devices (D, TVMD, TID and IPD) can be respectively calculated as

$$Y(s) = c,\ Y(s) = \frac{k(bs + c)}{bs^2 + cs + k},\ Y(s) = \frac{bs(cs + k)}{bs^2 + cs + k},\ Y(s) = bs + c \tag{3}$$

In [34], using a fixed-sized-inerter admittance — four configurations, the damper, the IPD, the TID and the TTID (shown in Figure 6(b) in [34]) — were found to be the optimal structures for reducing

Prepared using stcauth.cls
DOI: 10.1002/stc

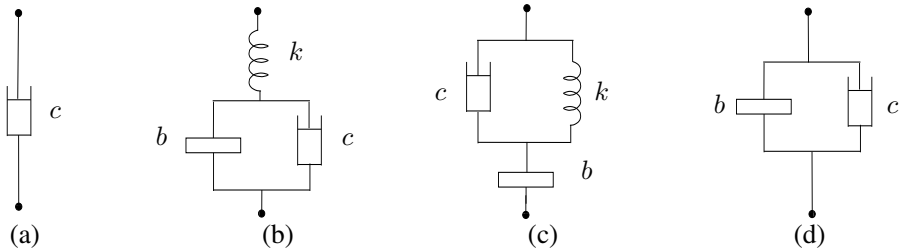

Figure 2. Four kinds of suppression layouts: (a) the damper (D), (b) the TVMD, (c) the TID and (d) the IPD.

the vibration for different regions making up the inertance-brace stiffness parametric space. Also it was found that the TTID was a sub-optimal structure since, for the region where it outperformed the other layouts, the resulting cost function could be matched or bettered by reducing either the inerter's size or the damping value. Hence, in this paper, candidate layouts 2D, 2TVMD and 2TID are considered; e.g., 2D means one damper at the bottom and the other damper mounted between the first and second floors of the building model. For the sake of comparison, the performance of each single device shown in Figure 2(a-c) located in the bottom storey will be analysed as well. The admittance functions $Y(s)$ obtained in (3) will be used to derive the objective function J_∞ for optimisation.

3. LIMITATION OF FIXED-SIZED-INERTER OPTIMISATION

A fixed-sized-inerter optimisation is carried out, where the inertance of the layouts is selected before optimisation. The range of the inerter's size considered in this paper is $b \in [100\text{ kg}, 3000\text{ kg}]$, i.e. $b/m_s \in [0.1, 3]$. For the single device mounted at the bottom, the optimum results of the damper, the TVMD and the TID have been shown in Figure 3(a), respectively. It can be seen that the TVMD provides the best performance over the whole range of inerter's size, slightly better than that of a damper. Comparing with the TID, the TVMD can have up to 93.1% performance improvement when $b = 100$ kg and the improvement percentage decreases with the increasing inerter's size, falling to 26.7% when $b = 3000$ kg.

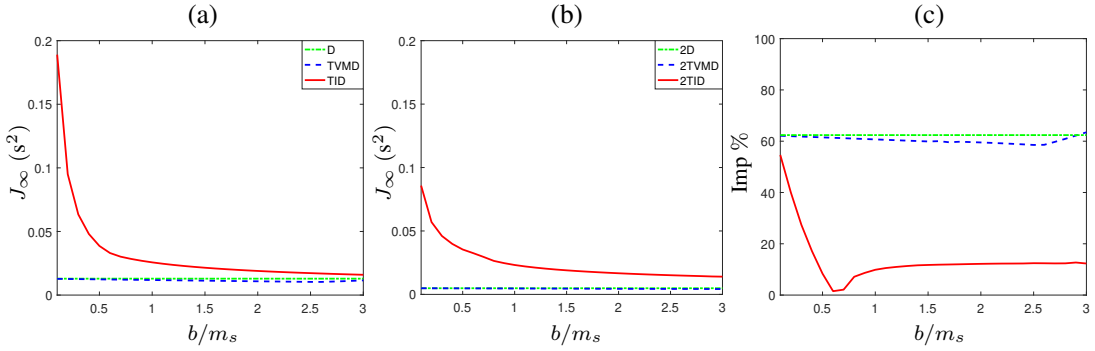

Figure 3. The optimisation results for minimising J_∞ over all device parameters: (a) a single device, (b) a pair of devices and (c) the percentage improvement of using two devices over a single one for the layouts D (green dash dotted), TVMD (blue dashed) and TID (red).

Considering a pair of vibration suppression devices, the selected inertance is split between the two inerters, with the ratio of split being one of the optimisation parameters. Figure 3(b) shows the optimal values of the objective function J_∞ with the layouts 2D, 2TVMD and 2TID. We observe that the 2TVMD provides the best performance over the whole range of inerter values considered, with up to 94.3% and 13.1% performance improvement comparing with the 2TID and 2D layouts, respectively. From Figure 3(a), (b), it can be noticed that a pair of devices can

DOI: 10.1002/stc

give significantly smaller values of the objective function J_∞. The percentage improvement with two absorbers has been shown in Figure 3(c), comparing with the corresponding single device. It suggests that the 2TVMD perform much better than a single TVMD in the whole range of the inerter's size, with around 62% improvement. For the 2TID layout, comparing with the single TID, the improvement is greatest at small inertance and decreases until $b \approx 600$ kg and over the range $b \in [1000\text{ kg},\ 3000\text{ kg}]$, the improvement percentage is always around 12%. The 2D layout can result in 62.4% smaller value of J_∞, comparing with a single damper.

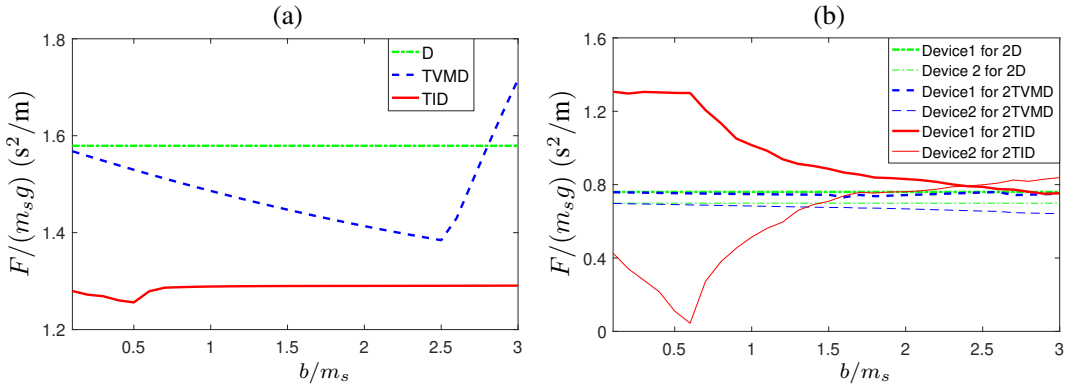

Figure 4. Device forces for (a) a single device with the TID (red), the D (green dash dotted) and the TVMD (blue dashed), (b) a pair of devices with the 2TID (red), the 2TVMD (blue dashed) and the 2D (green dash dotted), where thick line represents the force of Device1 and the thin one is that of Device2.

Forces exerted by the devices are also of interest for the optimal design of the vibration suppression devices. Figure 4 shows the force F for all the absorber layouts with the optimum parameter values for each value of b, where F is defined as

$$F = \max_{\omega} |T_{A_g \to F_d}(j\omega)| \tag{4}$$

which is the maximum magnitude of the transfer function from ground acceleration A_g to the device force F_d. From Figure 4 (a), it can be noticed that although the TVMD and the damper can result in better performance than the TID, the exerted forces of these three devices are in the same level. For the multiple devices considered, similar conclusions can be drawn from Figure 4(b).

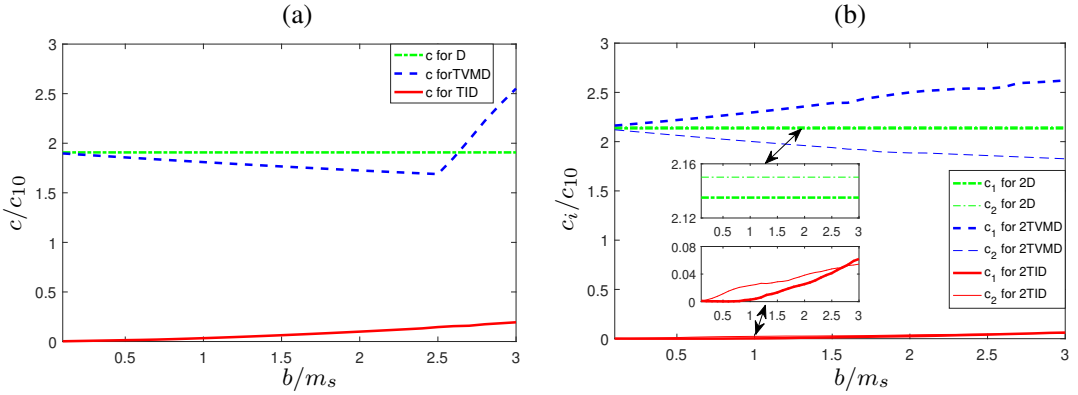

Figure 5. The optimal damping values for: (a) a single device, (b) a pair of devices with the structures D (green dash dotted), TVMD (blue dashed), TID (red).

The optimal damping values, nondimensionalized by a damping value $c_{10} = 76.4$ kNs/m, for a single and a pair of devices are given in Figure 5(a) and (b), respectively. The damping value c_{10} is

DOI: 10.1002/stc

calculated by:

$$c_{10} = \frac{10\% \times 2 \times \sqrt{m_{m1} k_{m1}}}{\phi_{1,1}^2}.$$

where $m_{m1},\ k_{m1}$ are the modal mass and modal stiffness of the first vibration mode of the building model, $\phi_{1,1}$ is the first component of the first mode shape. Assuming that only the contribution of the first vibration mode is significant, c_{10} represents the damping coefficient that provides a 10% damping ratio of the first mode if a pure damper is installed within the bottom storey. It should be noted that, for a pair of devices, the damping values for Device1 are represented by thick lines while those for Device2 are plotted in thin lines. From Figure 5(a), it can be seen that the damping value required for the TID is much smaller than that of both the TVMD and the damper, of which the optimal damping values are almost twice the value of c_{10}. Figure 5(b) suggests that although the devices (2TVMD and 2D) can achieve a smaller value of the objective function, the damping values of them are significantly larger than that of the 2TID layout. Comparing with the single device, the damping values of the 2TID are similar to that of the TID while the 2TID can achieve a better performance. It is known that damping devices have realistic range of effective damping values, related with fluid and valve designs [43]. In order to make meaningful and fair comparisons among the proposed candidate layouts, the damping limit on a single or a pair of devices will need to be implemented. In this work, we select c_{10} as the maximum damping limit, which is in line with that used by other researchers; for example, to illustrate the performance benefit of the TVMD, Ikago [31] compared it with a traditional damper using the same damping ratio for a single degree of freedom model, and the maximum damping ratio considered is 10%. In subsequent optimisation, we impose a bound on the sum of the damping coefficients added to the main structure. Similar work on restricting damping elements, especially the sum of the damping coefficient has been conducted by many researchers for identifying optimal suppression devices in building structures, e.g., [18, 44–46].

4. OPTIMISATION RESULTS WITH DAMPING RESTRICTION

This section reports the optimisation results when restricting the upper bound on the damping values required. The total inertance b is selected before optimisation and the total damping values should not exceed the proposed damping up-boundary, denoted as c_u. For the candidate layouts 2TID and 2TVMD, the parameters for optimisation are inertance ratio u_b with $u_b = b_1/b$, the damping values $c_1,\ c_2$ satisfying the condition $c_1 + c_2 \leq c_u$ and the stiffnesses $k_1,\ k_2$. The subscripts 1 and 2 relate to components in Device1 and Device2, respectively. As c_{10} is considered as the maximum upper bound for the total damping size added to the main structure, to show performance and optimal configuration trends when applying different damping constraints c_u ($c_u \leq c_{10}$), three example damping upper limits are analysed: $c_u = c_{10}/16$, $c_u = c_{10}/5$ and $c_u = c_{10}$.

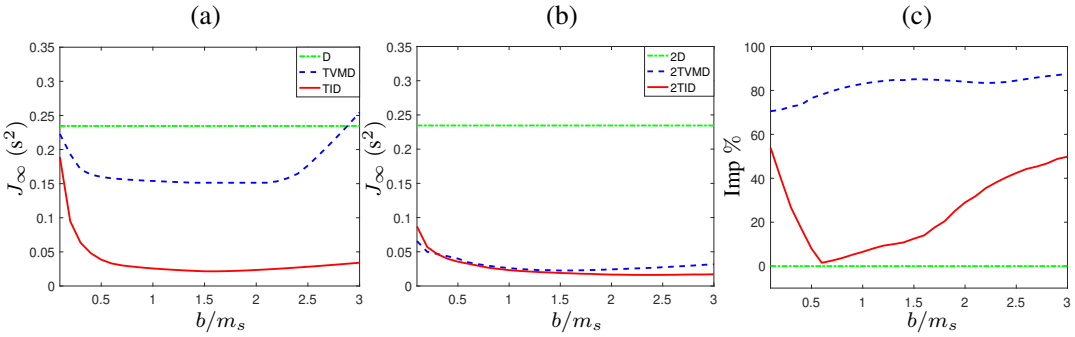

Figure 6. The optimisation results for $c_u = c_{10}/16$: (a) a single device, (b) a pair of devices, (c) the percentage improvement of using two devices over a single one for the layouts D(green dash dotted), TVMD (blue dashed) and TID (red).

Prepared using stcauth.cls
DOI: 10.1002/stc

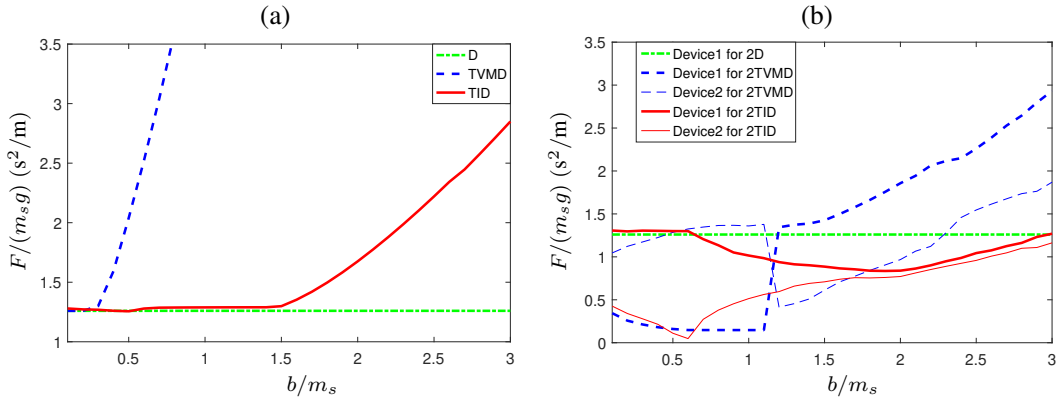

Figure 7. Device forces for $c_u = c_{10}/16$: (a) a single device with the TID (red), the D (green dash dotted) and the TVMD (blue dashed), (b) a pair of devices with the 2TID (red), the 2TVMD (blue dashed) and the 2D (green dash dotted), where thick line represents the force of Device1 and the thin one is that of Device2.

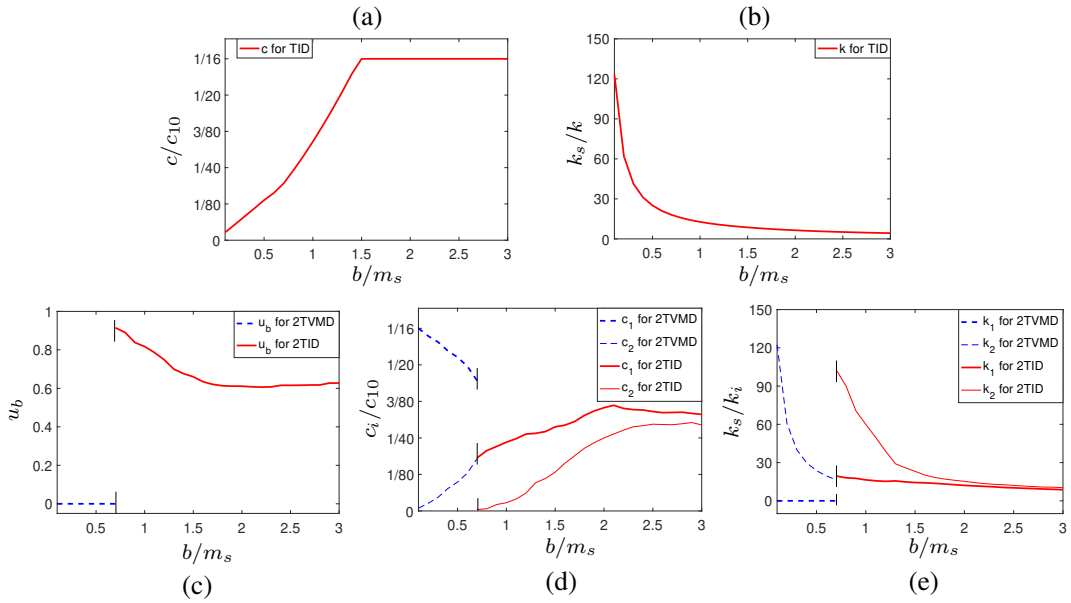

Figure 8. The corresponding optimal element values for $c_u = c_{10}/16$: for a single device (a) c, (b) k; for a pair of devices (c) the inertance ratio u_b, (d) c_1 (bold) and c_2 (thin), (e) k_1 (bold) and k_2 (thin) with the layouts TVMD (blue dashed), TID (red).

For the damping upper bound $c_u = c_{10}/16$, the optimum values of J_∞ using a single device and a pair of devices with three different devices shown in Figure 2 are given in Figure 6 (a) and (b), respectively. A comparison of the optimisation results between using a single device and a pair of devices is also given in terms of the percentage improvement in cost function using two devices of a certain layout over the use of one device of the same layout (see Figure 6 (c)). It can be seen from Figure 6(a) that, for the building model with a single device mounted at the bottom, the TID can provide the best performance over the whole range of inerter's size, significantly better than both the damper and the TVMD. Figure 6(b) shows that for two devices, the 2TVMD and the 2TID have different optimal inertance range, namely $b \in [100\text{ kg}, 700\text{ kg}]$ and $b \in (700\text{ kg}, 3000\text{ kg}]$, respectively. The percentage improvement in J_∞ of the pair of devices is presented in Figure 6(c); it can be seen that the 2D has the same performance with the single damper (over the whole inertance range). The 2TVMD gives a much smaller value of J_∞ comparing with a single TVMD and the relative improvement increases as the value of b increasing. Comparing with that of the

DOI: 10.1002/stc

TID, the smallest percentage improvement of the 2TID is 5.5%, which occurs when $b = 700$ kg. The maximum forces of the single device and a pair of devices are shown in Figure 7(a) and (b), respectively. It can be seen from Figure 7(a) that the damper provides the smallest force, while results in the worst suppression performance. The force of the TVMD increases rapidly with a larger value of b, while the TID has similar level of force as the damper. For the multiple devices, the exerted forces are all in the same level, as noted from Figure 7(b).

Figure 8 shows the optimal element values for the case $c_u = c_{10}/16$, but only showing where a particular suppression layout is optimal, with short vertical lines to note the transition points between layouts. For example, values for neither D nor 2D are shown in Figure 8 as they are not the optimal layout choices for any value of b in $[100 \text{ kg}, \ 3000 \text{ kg}]$. From Figure 8(a), it can be seen that the damping value of the single device TID in the range of $b \in [100 \text{ kg}, 1500 \text{ kg}]$ is smaller than the damping boundary $c_{10}/16$, which means, in this range, increasing the upper bound on the damping value will not result in improved TID performance. Figure 8(c) gives the inertance ratio u_b of the pair of devices, and from it, we note that the value of u_b for the 2TVMD is approximately zero when $b \in [100 \text{ kg}, 700 \text{ kg}]$. Also, over this range, the reciprocal value of the corresponding stiffness k_1 for the 2TVMD is almost zero. This suggests that for the 2TVMD layout, the lower device can be simplified to a damper in its whole optimal range of inerter's size and we denote this structure as DTVMD - a damper located at the bottom and a TVMD mounted between the first and second floors. Also note that the total optimal damping value of the 2TID is smaller than $c_{10}/16$ when b is less than 1900 kg.

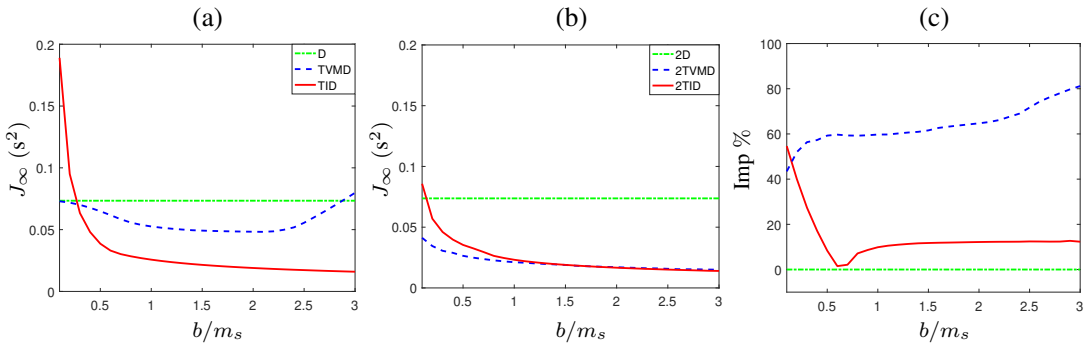

Figure 9. The optimisation results for $c_u = c_{10}/5$: (a) a single device, (b) a pair of devices, (c) the percentage improvement of using two devices over a single one for the layouts D(green dash dotted), TVMD (blue dashed) and TID (red).

The results in Figure 9, suggest that for the case $c_u = c_{10}/5$, the optimal range of the inerter's size for the TVMD and 2TVMD becomes larger as more damping is available. The optimal values of the cost function J_∞ with the TVMD and 2TVMD are much smaller than that for the case $c_u = c_{10}/16$. For the TID and 2TID layouts, comparing with the case $c_u = c_{10}/16$, the optimal results are the same in the range of $b \in [100 \text{ kg}, \ 1500 \text{ kg}]$ and $b \in [100 \text{ kg}, \ 1900 \text{ kg}]$, respectively. For a higher inertance, both the TID and 2TID can provide better performance. For the single device mounted at the bottom, it can be seen from Figure 9(a), the optimal configuration is the TVMD when $b \in [100 \text{ kg}, 300 \text{ kg}]$ and the TID over the remaining range. And from Figure 9(b), the optimal configuration for a pair of devices is 2TVMD and 2TID in the range of $b \in (100 \text{ kg}, 1700 \text{ kg}]$ and $b \in (1700 \text{ kg}, 3000 \text{ kg}]$, respectively. The performance improvement has also been shown in Figure 9(c), where 2D have the same performance with a damper. The 2TID achieves up to 52.1% improvement over the TID, while for the 2TVMD, the improvement over the TVMD increases as the inertance increases, with a 81% improvement when $b = 3000$ kg. Figure 10 suggests that the optimum suppression configurations in their corresponding optimal range of the inerter's size exert similar level of control forces. In addition, for the 2TID device, Device1 provides larger force than Device2, while in the optimal range of the 2TVMD, the TVMD located at the bottom exerts smaller force comparing with that located between the first and second floors.

DOI: 10.1002/stc

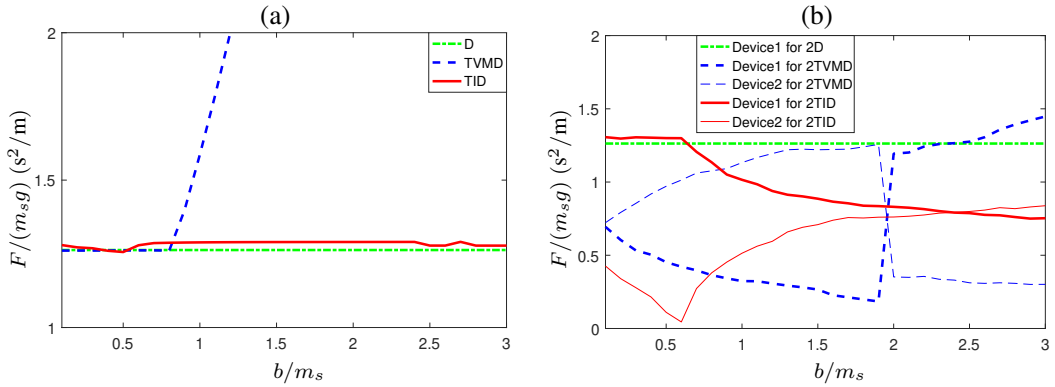

Figure 10. Device forces for $c_u = c_{10}/5$: (a) a single device with the TID (red), the D (green dash dotted) and the TVMD (blue dashed), (b) a pair of devices with the 2TID (red), the 2TVMD (blue dashed) and the 2D (green dash dotted), where thick line represents the force of Device1 and the thin one is that of Device2.

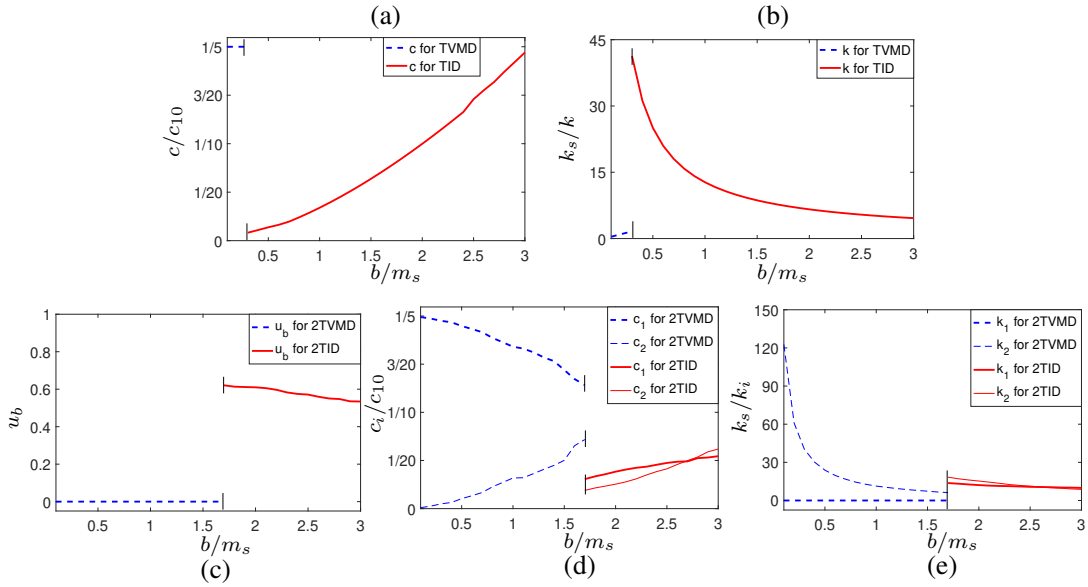

Figure 11. The corresponding optimal element values for $c_u = c_{10}/5$: for a single device (a) c, (b) k; for a pair of devices (c) the inertance ratio u_b, (d) c_1 (bold) and c_2 (thin), (e) k_1 (bold) and k_2 (thin) for a pair of devices with the layouts TVMD (blue dashed), TID (red).

The damper and spring values for the optimal TVMD and TID are shown in Figure 11(a) and (b). The optimal damping values of the TID is smaller than $c_{10}/5$ in the whole range of inerter's size. For the TVMD, the reciprocal value of the optimal stiffness of the TVMD is almost zero when b equals 100 kg, which means the TVMD can be reduced to a IPD, shown in Figure 2(d), at this inertance. For the case where a pair of devices is used, Figures 11(c) and (e) show that the 2TVMD can be simplified to the DTVMD when $b \in [100\text{ kg}, 1700\text{ kg}]$. From Figure 11(d), we notice that total damping values of the 2TID are smaller than the damping boundary $c_{10}/5$ in the whole range of the inerter's size, indicating that any damping boundary with larger value will not result in a better performance with the 2TID layout, this can be demonstrated in the following case $c_u = c_{10}$.

With the damping upper boundary set to c_{10}, Figure 12(a) shows that the TVMD outperforms the others when $b \in [100\text{ kg}, 2900\text{ kg}]$ and $b \in (2900\text{ kg}, 3000\text{ kg}]$ respectively. It can be noted from Figure 12(b) that the 2TVMD provides the best performance in the whole range of the inerter's size, with up to 83.9% and 46.4% improvement comparing with 2TID and 2D respectively. From Figure 9(b) and Figure 12(b), it can be seen that comparing with the previous case $c_u = c_{10}/5$, the

DOI: 10.1002/stc

value of J_∞ of 2TID is the same and that of 2TVMD and 2D is much smaller for the case $c_u =_{10}$. The comparison between a single device and a pair of devices with the damping restriction $c_u = c_{10}$ has been shown in Figure 12(c). From it, we can obtain that different from the previous cases, the improvement of 2D is about 2% comparing with the single damper. The 2TVMD still performs better than the TVMD, with 17.2%-52.9% improvement.

The device forces under this damping restriction are shown in Figure 13, also suggesting that all the devices result in similar levels of control force and the TVMD has much smaller force when the inerter's size is large, comparing with that for previous two damping limit cases. It can also be noted that different from the case that $c_u = c_{10}/5$, the TVMD located at the bottom has larger control force than the one mounted between the first and second floors in most range of inerter's size. The optimal stiffness for the TVMD is shown in Figure 14(b) and appears to be extremely large in the range of $b \in [100\text{ kg},\ 1600\text{ kg}]$, hence, the TVMD can again be simplified to the IPD. The inertance ratio and the optimal stiffness of the 2TVMD in Figure 14(c), (e) suggests that the 2TVMD can be reduced to the DTVMD in the whole range of the inerter's size.

Overall, we note that limiting the dampers' parameter has much less effect on the TID than the other layouts, as the TID typically requires much less damping whereas the TVMD and D appear to rely heavily on significant damping to achieve optimal performance. In addition, from Figures 7, 10 and 13, it can be noted that for a single damper with a higher damping, the exerted force becomes larger while the objective function becomes smaller. This shows a trade off between the lower value of the objective function J_∞ and lower control force F acting on the main structure. For the TID and TVMD, this trade off does not hold; for example, with a same inerter's size $b = 500$ kg, obtained from Figures 9 and 4, the force of TVMD is $F = 18$ kg with the cost function $J_\infty = 0.16$ s^2 when

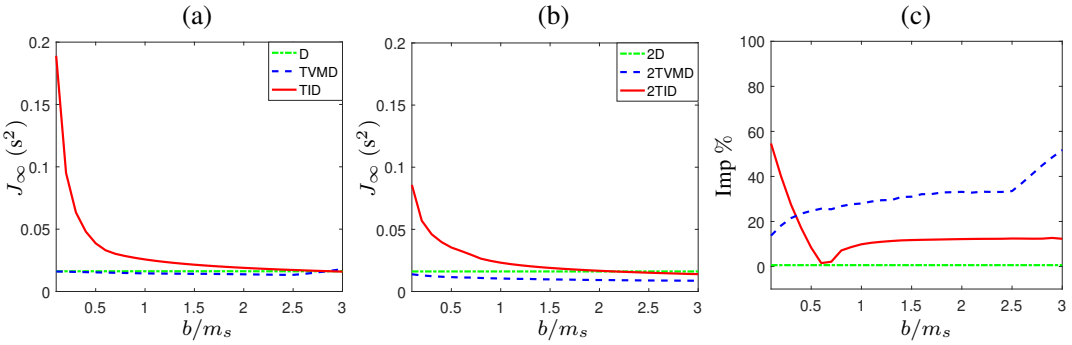

Figure 12. The optimisation results for $c_u = c_{10}$: (a) a single device, (b) a pair of devices, (c) the percentage improvement with the configurations D (green dash dotted), TVMD (blue dashed), TID (red).

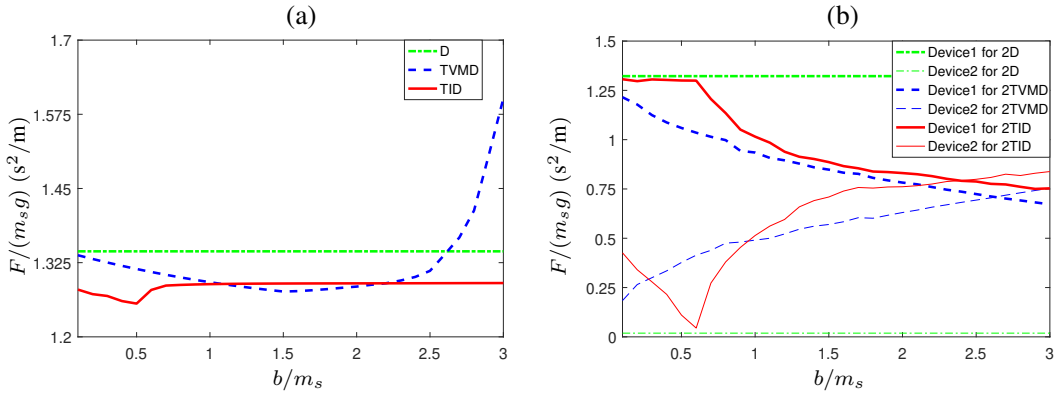

Figure 13. Device forces for $c_u = c_{10}$: (a) a single device with the TID (red), the D (green dash dotted) and the TVMD (blue dashed), (b) a pair of devices with the 2TID (red), the 2TVMD (blue dashed) and the 2D (green dash dotted), where thick line represents the force of Device1 and the thin one is that of Device2.

DOI: 10.1002/stc

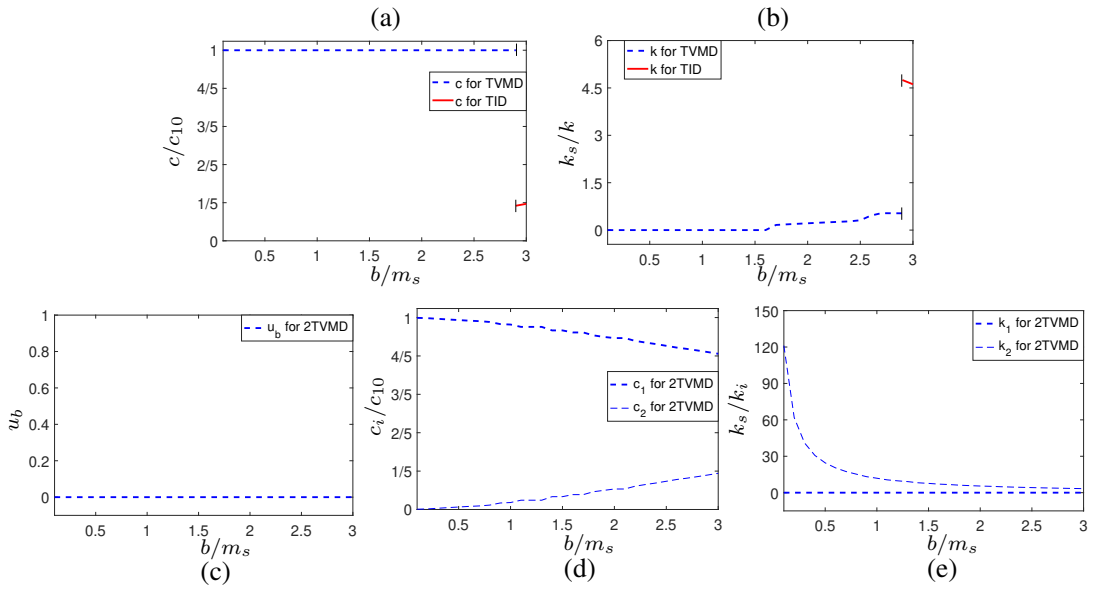

Figure 14. The corresponding optimal element values for $c_u = c_{10}$: for single device (a) c, (b) k; for a pair of device (c) the inertance ratio u_b, (d) c_1 (bold) and c_2 (thin), (e) k_1 (bold) and k_2 (thin) with the layouts TVMD (blue dashed), TID (red).

$c_u = c_{10}/16$, and based on Figures 9, 10, when $c_u = c_{10}/5$, we can obtain that $F = 12$ kg and $J_\infty = 0.07$ s^2. We can note that with the TID and the TVMD, a lower control force F can result in a lower value of J_∞. This is because for the TID and the TVMD, one additional degree of freedom is added to the primary structure and the performance resulted from such device is not only influenced by the acting force but also related to the movement of the added degree.

5. OVERALL BENEFICIAL LAYOUTS

From the analysis above, it can be concluded that the optimised layout is affected by the amount of inertance available and the upper bound of damping selected. With two devices, 2TVMD and 2TID always outperform the single device, the TVMD and TID, respectively. In contrast, the optimisation result of 2D is better than that of the single damper only when the damping boundary is large. In addition, the TVMD, 2TVMD can be reduced to the IPD, DTVMD over some range of the inerter's size for some upper damping limits.

Based on the conclusions obtained for the three specific damping boundary $c_u = c_{10}/16$, $c_u = c_{10}/5$ and $c_u = c_{10}$ with a single device and a pair of devices, we optimise the objective function with these proposed layouts for many damping restrictions in the range of $[0, c_{10}]$. The optimal regions with respect to the b value and the damping boundary for a single device and a pair of devices are shown in Figure 15(a) and (b), together with the optimisation results for the cost function. This will provide a guidance for selecting the appropriate configurations given a certain boundary for inertance, damping values and performance requirements. In some regions of the inerter's size and the damping boundary, the TVMD and 2TVMD are simplified to the IPD and DTVMD, respectively. It can be seen that using a pair of devices can provide a much better performance than the single device of equivalent inertance and damping boundary. From Figure 15(a), we notice that for some selected inerter's size, the optimisation result of the TID does not change when the damping boundary is higher than a specific value (see the vertical contour lines), this is because increasing the value of c_u does not result in a better performance. As a result, if limiting the value of the dampers' parameter is important, the TID is a preferable layout. Furthermore, it can be seen that for reducing the inter-storey drifts of a building model, both a single damper and a 2D do not

DOI: 10.1002/stc

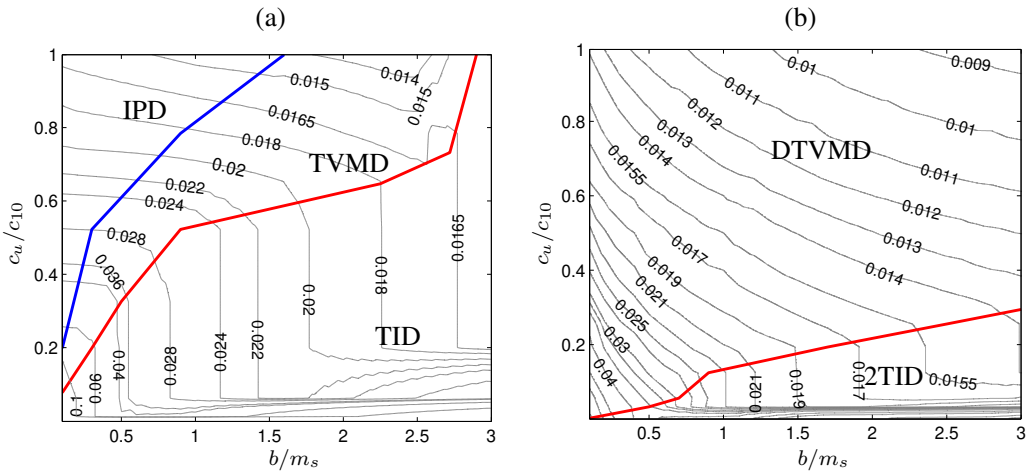

Figure 15. The optimal layouts and the optimisation results of J_∞ for (a) a single device and (b) a pair of devices.

provide superior performance comparing with the proposed inerter-based devices. The results in Figure 15(b), suggest that the DTVMD has a very large optimal region, where a bigger b and bigger c_u can always give a smaller value of J_∞. It can be also noted that the sensitivity of the DTVMD improves with the value of b and the damping boundary c_u increasing.

Finally, two illustrative numerical examples are conducted for demonstrating the results obtained in Figure 15, for selecting the optimal design of the suppression devices with given values of inerter b and damping up-boundary c_u. The actual values a designer might use will depend on a range of functions including practical acceptable device sizes, where the inerter's size is dependent on the physical inerter prototypes and the damping values are also needed to be constrained in a reasonable range, related with the fluid and valve design shown in Makris and Constantinou [43]. In terms of physical realisation, we take the inerter as an example. With a ball-screw inerter, the inertance is achieved by:

$$b = (\frac{2\pi}{P})^2 J$$

where P is the pitch of of the ball-screw assembly, J is the moment of inertia of the flywheel. It can be seen that by selecting smaller pitch values, the achieved inertance can be far greater than the actual mass of the device. For example, if $P = 5$ mm, to achieve a pre-determined value of the inertance b, the flywheel moment can be obtained as $J = 6.3 \times b \times 10^{-7}\text{kgm}^2$. Subsequently, based on this obtained moment, the dimensions the flywheel can be calculated, with which the ball-screw inerter can be designed and manufactured. For example, this could be achieved for $b = 2500$ kg using a 30 mm thick 90 mm diameter solid steel dish. Together with this ball-screw inerter, the optimum absorbers can then be assembled using the viscous damper and the coil spring. This approach has been adopted for realising the TVMD, and the manufactured prototype has been applied to a 14-storey building in Sendai, Japan [47].

We first consider an example that $b = 750$ kg and $c_u = 30.75$ kNs/m. Based on the Figure 15, it can be seen that the DTVMD is the optimal design for providing the smallest value of J_∞. To show the superiority of this device, three other devices, the D, the TVMD and the TID, with the same inertance $b = 750$ kg and the same damping up-boundary $c_u = 30.75$ kNs/m are analysed for a sake of comparison, with which, the optimisation results are summarised in Table I. It can be seen that comparing with the damper, the TID and the TVMD, the optimal device DTVMD can respectively provide 51%, 38% and 47% performance improvement. The control forces F have also been shown in Table I, suggesting that similar force levels are required for these four configurations. It can also be noted that for the single device, the TID results in a value of the objective function J_∞ as 0.029, which is in line with that obtained from Figure 15(a). Also note that at this point in b, c_u space, the TID provides better performance than the TVMD (14.7% improvement), as expected

DOI: 10.1002/stc

Table I. Optimisation results with the D, TID, TVMD and DTVMD when $b = 750$ kg and $c_u = 30.75$ kNs/m.

Configurations	J_∞, s^2	F, kNs^2/m	Optimum parameter values, kNs/m, kN/m
D	0.037	12.5	$c = 30.75$
TID	0.029	12.7	$c = 1.66,\ k = 89.03$
TVMD	0.034	12.4	$c = 30.75,\ k = 1689.6$
DTVMD	0.018	$F_1 = 6.21,\ F_2 = 7.79$	$c_1 = 29.27,\ c_2 = 1.48,\ k = 95.1$

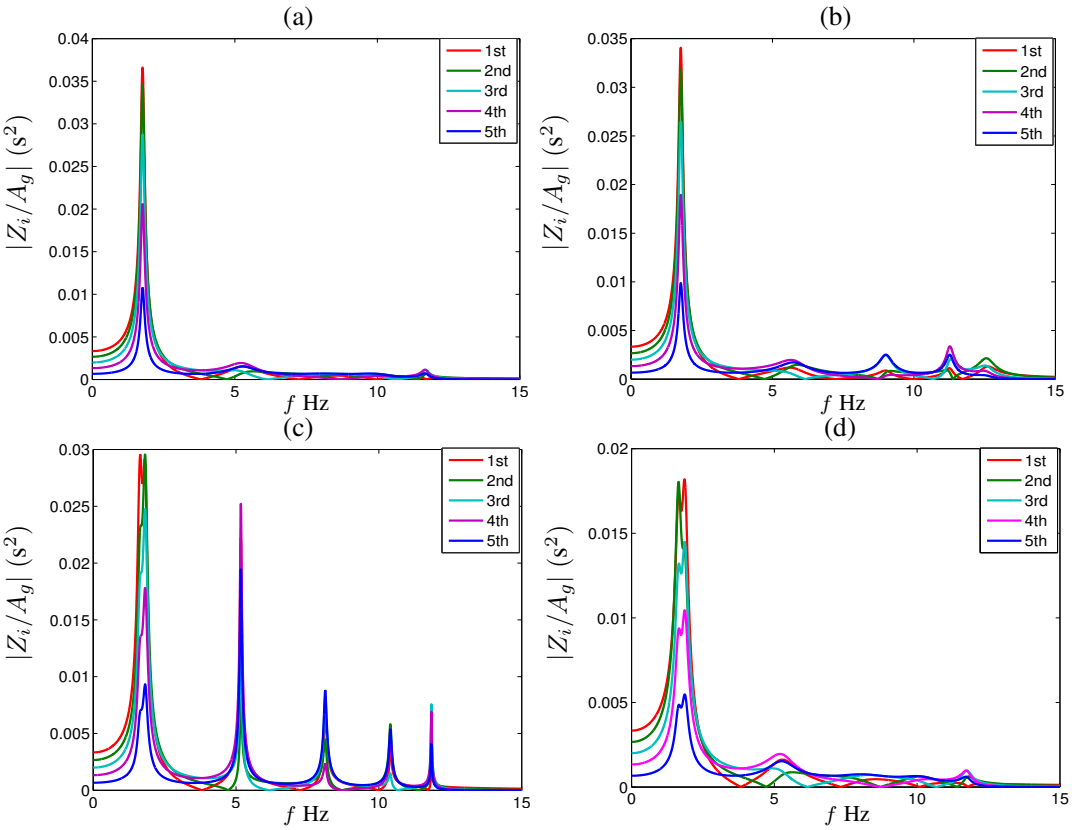

Figure 16. Magnitudes of frequency response functions from ground accelerations A_g to inter-storey drifts Z_i with (a) the damper (D), (b) the TVMD, (c) the TID and (d) the DTVMD when $b = 750$ kg and $c_u = 30.75$ kNs/m.

from Figure 15(a). Using the optimum parameter values obtained in Table I, the corresponding inter-storey drift frequency response of the building model is shown in Figure 16, from which, it can also be seen that the DTVMD provides the best performance.

To further verify the seismic performance of these four configurations, the five-storey building model with these devices is studied with respect to two earthquake base excitations, the JMA N-S Tohoku earthquake of March 11, 2011 with the duration as 180 s and the JMA N-S Kobe earthquake of January 17, 1995 with duration as 50 s. These two earthquakes are shown in Figure 17(a) and Figure 18(a), respectively. With both the earthquakes, Figures 17(b) and 18(b) illustrate the time response of the inter-storey drift between the first floor and the ground. It can be seen that all the devices D, TID, TVMD and DTVMD suppress the vibration and among these, the DTVMD provides the best performance over the whole time range, which is significantly better than the other devices. The TID, D and the TVMD have very similar performance under these two earthquake

DOI: 10.1002/stc

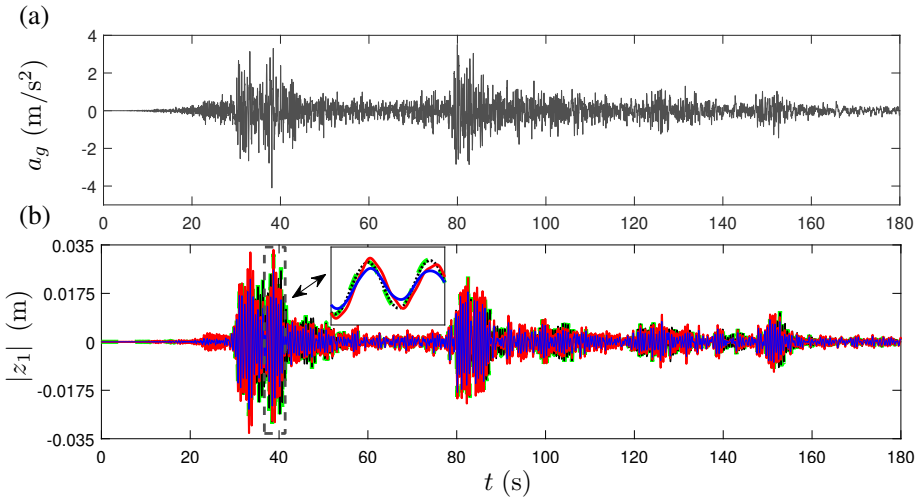

Figure 17. For the Tohoku earthquake: (a) Ground acceleration time-history and (b) first floor inter-storey drift time history with the D (green dashed), TID (red), TVMD (black dotted), DTVMD (blue) for $b = 750$ kg and $c_u = 30.75$ kNs/m.

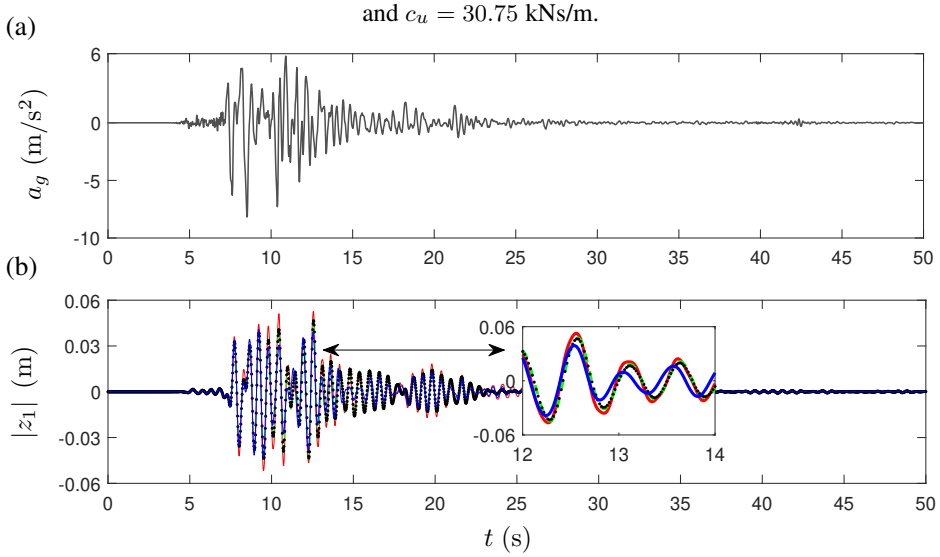

Figure 18. For the Kobe earthquake: (a) Ground acceleration time-history and (b) first floor inter-storey drift time history with the D (green dashed), TID (red), TVMD (black dotted), DTVMD (blue) for $b = 750$ kg and $c_u = 30.75$ kNs/m.

Table II. The peak value F_{max} and the root mean square value F_{rms} of the the exerted forces with the four devices subjected to Tohoku and Kobe earthquakes when $b = 750$ kg and $c_u = 30.75$ kNs/m.

Configurations	Tohoku earthquake				Kobe earthquake			
	F_{1max} (kN)	F_{2max} (kN)	F_{1rms} (kN)	F_{2rms} (kN)	F_{1max} (kN)	F_{2max} (kN)	F_{1rms} (kN)	F_{2rms} (kN)
D	9.78	–	1.65	–	16.1	–	2.94	–
TID	10.8	–	1.98	–	16.9	–	3.23	–
TVMD	10.4	–	1.75	–	17.3	–	3.05	–
DTVMD	7.22	8.30	1.16	1.31	14.8	11.5	2.41	2.33

DOI: 10.1002/stc

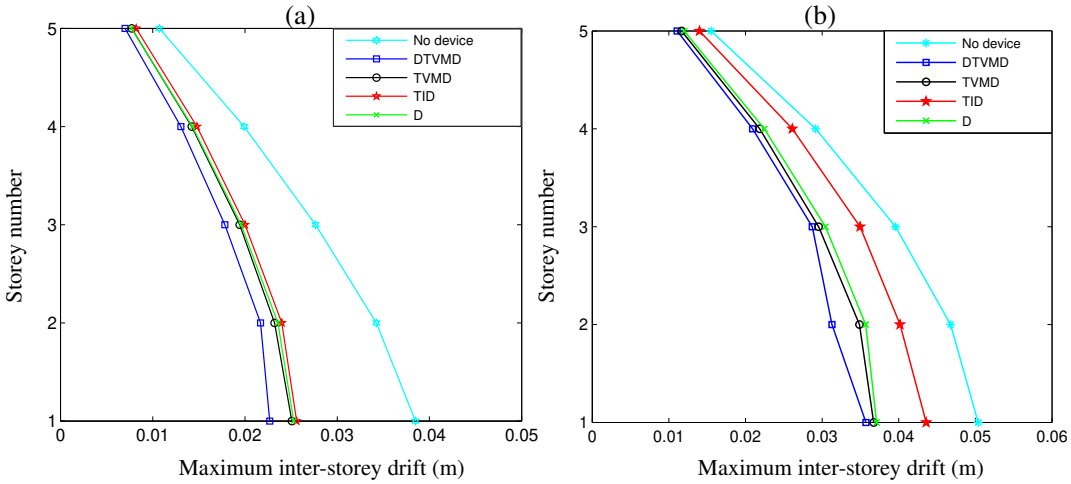

Figure 19. Maximum inter-storey drift for the building model with 3% structural damping ratio controlled by no device, DTVMD, TVMD, IPD and TID for $b = 750\,\mathrm{kg}$ and $c_u = 30.75$ kNs/m against (a) Tohoku earthquake, (b) Kobe earthquake.

excitations, as expected from Table I and Figure 16. The peak forces F_{max} and the root mean square value (RMS) of the exerted forces (F_{rms}) with these four configurations are summarised in Table II for the Tohoku and Kobe earthquakes, respectively. Note that these values are taken over the whole duration of the considered earthquakes, i.e. 180 s for Tohoku earthquake and 50 s for Kobe earthquake. It can be noted that under the Kobe earthquake, higher control forces are required comparing with the Tohoku earthquake and subjected to both these two earthquakes, all the four devices, the D, TID, TVMD and DTVMD, exert similar force levels, as expected from Table I. Also note that the maximum force exerted by the optimum device, the DTVMD, is 8.3 kN and 14.8 kN when the structure is subjected to the Tohoku and Kobe earthquakes, respectively. These are 16.6% and 30% of the structure weight, 49 kN. However, when comparing with the traditional damper with the same amount of damping, 30.75 kNs/m, the DTVMD results in not only the better performance but also the smaller force. Using these four configurations in a building model with 3% structural damping, the maximum drift between each two connected stories during the earthquake are shown in Figure 19 for both the Tohoku and the Kobe earthquakes. Comparing with the response for this building model with no device, these figures confirm that the proposed vibration suppression devices reduce the inter-storey drifts for all the floors and the DTVMD provides the best performance.

Table III. Optimisation results with the D, TID, 2TID and DTVMD when $b = 2500$ kg and $c_u = 20$ kNs/m.

Configurations	J_∞, s^2	F, $\mathrm{kNs}^2/\mathrm{m}$	Optimum parameter values, kNs/m, kN/m
D	0.056	12.4	$c = 20$
TID	0.017	12.5	$c = 11.14,\ k = 277.6$
2TID	0.015	$F_1 = 7.74,\ F_2 = 7.86$	$u = 0.57,\ c_1 = 3.62$ $k_1 = 139.8,\ c_2 = 3.16,\ k_2 = 132.9$
DTVMD	0.015	$F_1 = 1.82,\ F_2 = 12.3$	$c_1 = 9.98,\ c_2 = 10.02,\ k = 387.7$

The second example is to identify the optimal absorber with the constraints that the required inertance and damping constraint are $b = 2500$ kg and $c_u = 20$ kNs/m. From Figure 15(a), the approximate optimum control configuration of the single device is the TID. Figure 15(b) suggests that the DTVMD and the 2TID provide similar performance at this $b - c_u$ point. The optimum

DOI: 10.1002/stc

results for these three devices, the TID, the 2TID and the DTVMD are summarised in table III, where a single damper is also provided for comparison. The optimum result shows that the 2TID provides 11.8% performance improvement comparing with a single TID, and results in same value of J_∞ as the DTVMD. The drift frequency response of the building model with the four configurations are

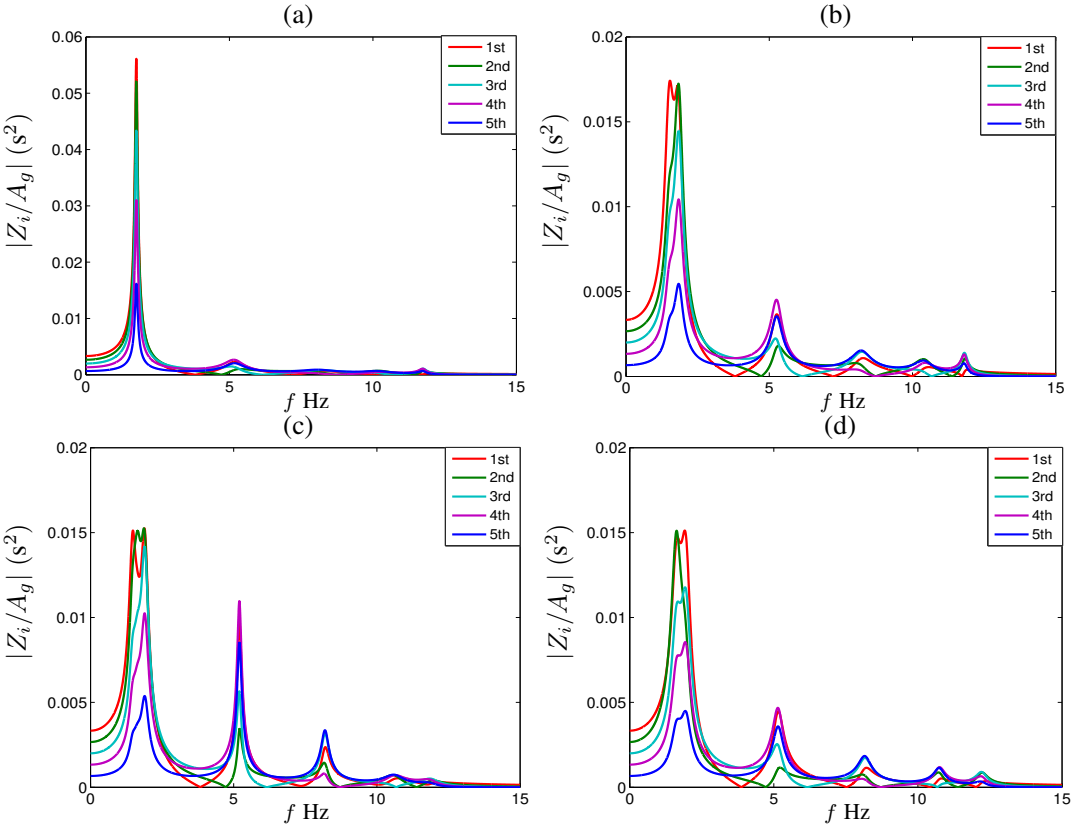

Figure 20. Magnitudes of frequency response functions from ground accelerations A_g to inter-storey drifts Z_i with (a) the damper (D), (b) the TID, (c) the 2TID and (d) the DTVMD when $b = 2500$ kg and $c_u = 20$ kNs/m.

Table IV. The peak value F_{max} and the root mean square value F_{rms} of the the exerted forces with the four devices subjected to Tohoku and Kobe earthquakes when $b = 2500$ kg and $c_u = 20$ kNs/m.

Configurations	Tohoku earthquake				Kobe earthquake			
	F_{1max} (kN)	F_{2max} (kN)	F_{1rms} (kN)	F_{2rms} (kN)	F_{1max} (kN)	F_{2max} (kN)	F_{1rms} (kN)	F_{2rms} (kN)
D	7.93	–	1.38	–	11.6	–	2.25	–
TID	17.1	–	2.45	–	28.6	–	5.06	–
2TID	11.2	8.47	1.51	1.38	18.7	15.3	3.40	2.74
DTVMD	3.01	15.1	0.40	2.37	5.47	29.2	0.83	4.89

shown in Figure 20, suggesting the similar conclusions obtained in Table III. Table IV summarises the forces exerted by the three inerter-based devices, together with the traditional damper for the case that $b = 2500$ kg, $c_u = 20$ kNs/m. It can be seen that the DTVMD exerts the maximum

DOI: 10.1002/stc

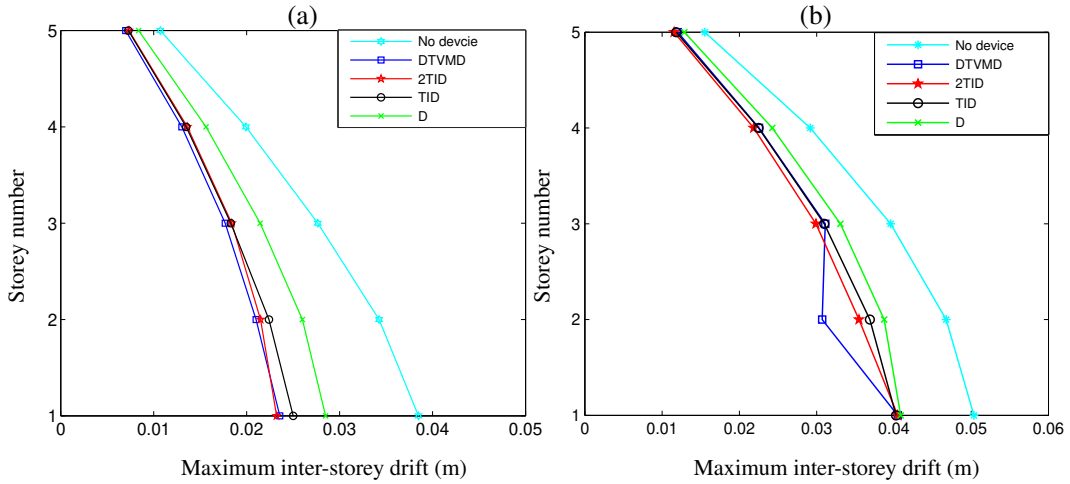

Figure 21. Maximum inter-storey drift for the building model with 3% structural damping ratio controlled by no device, DTVMD, 2TID, D and TID for $b = 2500\,\mathrm{kg}$ and $c_u = 20$ kNs/m against (a) Tohoku earthquake, (b) Kobe earthquake.

force $F_{2\max} = 29.2$ kN for the Kobe earthquake, approximately 60% of the structure weight, which is a significant large force acting on the structure. The 2TID device provides similar seismic performance (see Table III and Figure 20), but results in much smaller maximum forces. Hence, the 2TID device is considered as the optimum vibration suppression device. The maximum inter-storey drifts for a building model with 3% structural damping ratio subjected to the two earthquakes are also obtained in Figure 21, demonstrating the effectiveness of the optimum device, the 2TID.

6. CONCLUSIONS

The main focus of this paper is to identify the potential benefits of using two inerter-based suppression devices over the use of a single device. Three layouts mounted between the ground and the first, and the first and second floors of a building model are taken into consideration. For the sake of comparison, a single device located between the ground and the first floor is also considered. Results from fixed-sized-inerter optimisations are presented to demonstrate that the value of damper(s) in the devices can be very large in some cases. Hence, to form a fair comparison, and also to take limitations for physical implementation into consideration, analysis with damping constraints are conducted. Using the maximum magnitude across all the inter-storey drifts and across the whole frequency as the cost function, an optimisation procedure is carried out for fixed inertance and with a limit on the maximum damping imposed. As a result, the optimum layouts and the optimal results for a single and a pair of suppression devices have been obtained with respect to the different inerter's size and different up boundaries of the damping value limits, respectively. It has been shown that comparing with the single suppression device, a pair of devices can always provide better performance with the same inertance and damping constraints. Furthermore, the TID requires much less damping to result in the optimal performance compared to the TVMD or the damper layouts, and so becomes the optimal configuration over a wide range of acceptable inertance as the constraint on the damping is lowered. Finally, the frequency responses were presented to show the validity of the proposed optimal configurations. The approach taken in this work is applicable for investigation of the case where multiple devices are used.

ACKNOWLEDGEMENTS

The authors would like to acknowledge the support of the EPSRC, the University of Bristol and the China Scholarship Council: S.A.Neild is supported by an EPSRC fellowship EP/K005375/1, Sara Ying Zhang is

supported by a University of Bristol studentship and the China Scholarship Council. Jason Zheng Jiang is supported by an EPSRC grant EP/P103456/1.

REFERENCES

1. Frahm H. Device for damping vibrations of bodies 1909.
2. DenHartog JP. *Mechanical Vibration*. McGraw Hill: York, PA, USA, 1940.
3. Fujino Y, Abe M. Design formulas for tuned mass dampers based on a perturbation technique. *Earthquake Engineering and Structural Dynamics* 1993; **22**:833–854.
4. Moutinho C. An alternative methodology for designing tuned mass dampers to reduce seismic vibrations in building structures. *Earthquake Engineering and Structural Dynamics* 2012; **41**:2059–2073.
5. Angelis MD, Perno S, Reggio A. Dynamic response and optimal design of structures with large mass ratio TMD. *Earthquake Engineering and Structural Dynamics* 2012; **41**:41–60.
6. Krenk S. Frequency analysis of the tuned mass damper. *Journal of Applied Mechanics* 2005; **72**:936–942.
7. Villaverde R. Reduction in seismic response with heavily-damped vibration absorbers. *Earthquake Engineering and Structural Dynamics* 1985; **13**:33–42.
8. Sadek F, Mohraz B, Taylor AW, Chung RM. A method of estimating the parameters of tuned mass damper for seismic applications. *Earthquake Engineering and Structural Dynamics* 1997; **26**:617–635.
9. Iwanami K, Seto K. Optimum design of dual tuned mass dampers and their effectiveness. *Proceedings of the JSME(C)* 1984; **50**:44–52.
10. Li C. Performance of multiple tuned mass dampers for attenuating undesirable oscillations of structures under the ground acceleration. *Earthquake Engineering and Structural Dynamics* 2000; **29**:1405–1421.
11. Igusa T, Xu K. Vibration control using multiple tuned mass damper. *Joural of Sound and Vibration* 1994; **175**:491–503.
12. Kareem A, Kline S. Performance of multiple mass dampers under random loading. *Journal of Structural Engineering* 1995; **121**:348–361.
13. Moon KS. Vertically distributed multiple tuned mass dampers in tall buildings: performance analysis and preliminary design. *The Structural Design of Tall and Special Buildings* 2010; **19**:347–366.
14. Fu TS, Johnson EA. Distributed mass damper system for integrating structural and environmental controls in buildings. *Journal of Engineering Mechanics* 2011; **137**:205–213.
15. Tong X, Zhao XW. Vibration suppression of the finite-dimensional approximation of the non-uniform SCOLE model using multiple tuned mass dampers. IEEE 55th Conference on Decision and Control (CDC), 2016.
16. Rana R, Soong T. Parametric study and simplified design of tuned mass dampers. *Engineering Structures* 1998; **20**:193–204.
17. Xiang P, Nishitani A. Seismic vibration control of building structures with multiple tuned mass damper floors integrated. *Earthquake Engineering and Structural Dynamics* 2014; **43**:909–925.
18. Takewaki I. Optimal damper placement for minimum transfer functions. *Earthquake Engineering and Structural Dynamics* 1997; **26**:1113–1124.
19. Smith MC. Synthesis of mechanical networks: the inerter. *IEEE Transactions on Automatic Control* 2002; **47**:1648–1662.
20. Papageorgiou C, Smith MC. Positive real synthesis using matrix inequalities for mechanical networks: application to vehicle suspension. *IEEE Transactions on Control Systems Technology* 2006; **14**:423–435.
21. Smith MC, Wang FC. Performance benefits in passive vehicle suspensions employing inerters. *Vehicle System Dynamics* 2004; **42**:235–237.
22. Smith MC. http://www.eng.cam.ac.uk/news/stories/2008/mclaren [19 August,2008].
23. Evangelou S, Limebeer DJN, Sharp RS, Smith MC. Mechanical steering compensation for high-performance motorcycles. *Journal of Applied Mechanics* 2007; **74**:332–346.
24. Jiang JZ, Smith MC, Houghton NE. Experimental testing and modelling of a mechanical steering compensator. *The 3rd International Symposium on Communications, Control and Signal Processing (ISCCSP)*, 2007.
25. Wang FC, Liao MK, Liao BH, Su WJ, Chan HA. The performance improvements of train suspension systems with mechanical networks employing inerters. *Vehicle System Dynamics* 2009; **47**:805–830.
26. Jiang JZ, Matamoros-Sanchez AZ, Goodall RM, Smith MC. Passive suspensions incorporating inerters for railway vehicles. *Vehicle System Dynamics* 2011; **50**:263–276.
27. Li Y, Jiang JZ, Neild S. Inerter-based configurations for main landing gear shimmy suppression. *Journal of Aircraft* 2016; doi:10.2514/1.C033964.
28. Zhu M, Zhang S, Jiang J, Macdonald J, Neild S. Enhancing the dynamic performance of a pantograph-catenary system via inerter-based damping technology. International Conference on Noise and Vibration Engineering, 2018.
29. Li Y, Zhang S, Jiang J, Neild S, Ward I. Passive vibration control of offshore wind turbines using the structure-immittance approach. International Conference on Noise and Vibration Engineering, 2018.
30. Wang F, Su W, Chen C. Building suspensions with inerters. *Proceedings of the Institution of Mechanical Engineers, Part C, Journal of Mechanical Engineering Science* 2010; **224**:1650–1616.
31. Ikago K, Saito K, Inoue N. Seismic control of single-degree-of-freedom structure using tuned viscous mass damper. *Earthquake Engineering and Structural Dynamics* 2012; **41**:453–474.
32. Lazar IF, Neild SA, Wagg DJ. Using an inerter-based device for structural vibration suppression. *Earthquake Engineering and Structural Dynamics* 2014; **43**:1129–1147.
33. Marian L, Giaralis A. Optimal design of a novel tuned mass-damper-inerter (TMDI) passive vibration control configuration for stochastically support-excited structural systems. *Probabilistic Engineering Mechanics* 2014; **38**:156–164.
34. Zhang SY, Jiang JZ, Neild SA. Optimal configurations for a linear vibration suppression device in a multi-storey building. *Structural Control and Health Monitoring* 2016; **24**, doi:10.1002/stc.1887.

35. Lu L, Duan YF, Jr BS, Lu X, Zhou Y. Inertial mass damper for mitigating cable vibration. *Structural Control and Health Monitoring* 2016; doi:10.1002/stc.1986.
36. Gonzalez-Buelga A, Lazar IF, Jiang JZ, Neild SA, Inman DJ. Assessing the effect of nonlinearities on the performance of a tuned inerter damper. *Structural Control and Health Monitoring* 2016; **33**, doi:10.1002/stc.1879.
37. Ikago K, Sugimura Y, Saito K, Inoue N. Seismic displacement control of multiple-degree-of-freedom structures using tuned viscious mass dampers. *Proceedings of the 8th International Conference on Structural Dynamics*, Leuven, Belgium, 2011.
38. Takewaki I, Murakami S, Yoshitomi S, Tsuji M. Fundamental mechanism of earthquake response reduction in building structures with inertial dampers. *Structural Control and Health Monitoring* 2012; **19**:590–608.
39. Giaralis A, Marian L. Use of inerter devices for weight reduction of tuned-mass-dampers for seismic protection of multi-story building: the tuned mass-damper-interter (TMDI). *SPIE 9799, Active and Passive Smart Structures and Integrated Systems* 2016; doi:10.1117/12.2219324.
40. Warburton GB. Optimum absorber parameters for various combinations of response and excitation parameters. *Earthquake Engineering and Structural Dynamics* 1982; **10**:381–401.
41. Shearer JL, Murphy AT, Richardson HH. *Introduction to system dynamics*. Addison-Wesley: USA, 1967.
42. Xiang P, Nishitani A. Optimum design of tuned mass damper floor system integrated into bending-shear type building based on H_∞, H_2, and stability maximization criteria. *Structural Control and Health Monitoring* 2015; **22**:919–938.
43. Makris N, Constantinou M. Viscous dampers: Testing, modeling and application in vibration and seismic. *NCEER-90-0028, National Center for Earthquake Engineering Research*, 1990.
44. Singh M, Moreschi L. Optimal seismic response control with dampers. *Earthquake Engineering and Structural Dynamics* 2001; **30**:553–572.
45. Trombetti T, Silvestri S. On the modal damping ratios of shear-type structures equipped with Rayleigh damping systems. *Journal of Sound and Vibration* 2006; **292**:21–58.
46. Trombetti T, Silvestri S. Novel schemes for inserting seismic dampers in shear-type systems based upon the mass proportional component of the Rayleigh damping matrix. *Journal of Sound and Vibration* 2007; **302**:486–526.
47. Chen Z, Junya K, Masahiro I, Kohju I, Norio I. Viscoelastically supported viscous mass damper incorporated into a seismic isolation system. *Journal of Earthquake and Tsunami* 2016; **10**, doi:10.1142/S1793431116400091.